



# Regressive Erosion at River Coca in Northeast Ecuador: Landslide Monitoring with Sentinel-1 to Support Disaster Risk Management

Valerie Graw<sup>1,2,3</sup>  · Torben Dedring<sup>1</sup> · Roman Hiby<sup>1</sup> · Jose Jara-Alvear<sup>2,3,4</sup> · Pablo Guzman<sup>2,3,4</sup> · Carsten Juergens<sup>1</sup>

Received: 28 February 2022 / Accepted: 22 September 2022 / Published online: 20 October 2022  
© The Author(s) 2022

## Abstract

After the collapse of the San Rafael waterfall in Northeast Ecuador on 2 February 2020, a regressive erosion started along the River Coca putting national infrastructure, the environment and indigenous communities at risk. A fast monitoring of areas exposed to landslides on local scales therefore is necessary to provide adequate risk management for the region. The study area, located in the Andean tropics close to the volcano Reventador, is characterized by steep slopes, seismic activity and high rainfall throughout the year. Sentinel-1 SAR data provide a solution for time-series monitoring in the region as imagery is available day and night and not affected by cloud cover. Landslide monitoring with Sentinel-1 SAR data was implemented using a bi-temporal change detection (BCD) with SNAP and a sequential change detection (SCD) with EESA Docker and the Google Earth Engine (GEE) aiming at the identification of a suited approach for fast disaster monitoring and management. The SCD showed an overall accuracy of 0.91 compared to 0.88 using the BCD approach validated with high-resolution imagery. Based on the landslide detection, hazard variables could be further identified to support future hazard and risk assessment. Fast processing of Sentinel-1 time-series data in a cloud-based environment allows for near real-time monitoring of ongoing erosion and provides a potential for pro-active measures to protect the national economy, the environment and the society.

**Keywords** Landslide monitoring · Sentinel-1 · Regressive erosion · Disaster risk management

## Zusammenfassung

*Regressive Erosion am Rio Coca in Nordost Ecuador – Hangrutschungs-Monitoring mit Sentinel-1 zur Unterstützung des Katastrophenrisikomanagements.* Nach dem Zusammenbruch des San Rafael Wasserfalls im Nordosten Ecuadors am 2. Februar 2020, begann eine regressive Erosion entlang des Rio Coca, welche die nationale Infrastruktur, die Umwelt sowie indigene Gemeinschaften bedrohte. Lokales Nahechtzeit-Monitoring des für Hangrutschungen exponierten Areals, ist daher notwendig um ein angepasstes Risikomanagement für die Region zu entwickeln. Das Untersuchungsgebiet rundum den Vulkan Reventador in den andinischen Tropen ist durch steile Hänge, seismische Aktivitäten und hohe Niederschläge über das ganze Jahr gekennzeichnet. Für ein zeitlich hoch aufgelöstes Monitoring der Region sind Sentinel-1 SAR Bilder geeignet, da sie Tag und Nacht und bei Bewölkung zur Verfügung stehen. In dieser Studie wurde eine Hangrutschungsdetektion mit Sentinel-1-Daten durchgeführt, wobei eine bi-temporale Veränderungsdetektion (BCD) in SNAP mit einer sequenziellen Veränderungsdetektion (SCD) mit EESA Docker und der Google Earth Engine (GEE) verglichen wurde. Die SCD zeigte eine Gesamtgenauigkeit von 0,91 verglichen mit einer Gesamtgenauigkeit von 0,88 mit dem BCD Ansatz. Beide Ansätze wurden mit hochaufgelösten multispektralen Bilddaten validiert. Basierend auf der Detektion der Hangrutschungen konnten des Weiteren Variablen identifiziert werden, die für das Gefahrenmonitoring für zukünftige Risikobewertungen eingesetzt werden können. Ein schnelles Prozessieren von Sentinel-1 Zeitreihen in einer cloud-basierten Umgebung erlaubt somit das Nahechtzeit-Monitoring der permanenten Erosion und zeigt Potenziale für proaktive Messungen um die nationale Wirtschaft, die Umwelt und die Gemeinschaften vor Ort zu schützen.

✉ Valerie Graw  
valerie.graw@rub.de

<sup>1</sup> Geomatics Research Group (GRG), Ruhr-University Bochum (RUB), Bochum, Germany

<sup>2</sup> Transdisciplinary Center for Coupled Socio-Ecological Systems (TRACES), Universidad del Azuay (UDA), Cuenca, Ecuador

<sup>3</sup> Energy Sciences Research Group (CIENER), Universidad del Azuay (UDA), Cuenca, Ecuador

<sup>4</sup> La Corporación Eléctrica del Ecuador (CELEC EP), Cuenca, Ecuador

## 1 Introduction

The number of disasters in the Americas has increased exponentially (Tsuneki et al. 2017). In Ecuador, the rate of damage caused by natural hazards is higher than the world average and the country is highly exposed to natural hazards in South America (Greiving et al. 2021). About 73.6% of the Ecuadorian population is exposed to two or more natural hazards (Dilley et al. 2012). Landslide hazards are expected to increase in frequency and intensity in the country due to climate change and infrastructure vulnerability (Carvajal et al. 2017; Sepúlveda and Petley 2015). The main causative factors for their occurrence are caused by its location in the Pacific Ring of Fire and further triggered by the El Niño Southern Oscillation (ENSO) (EM-DAT 2022). Landslides frequently occur in the country due to the combined effects of high seismic activity and the tropical mountain environment with steep slopes, high variability in hydrological patterns and increasing land pressure especially in the steep uplands in addition (Guns and Vanacker 2013; Tibaldi et al. 1995).

On 2 February 2020, the biggest waterfall of Ecuador, San Rafael, collapsed due to an unusual erosion phenomenon caused by volcanic debris avalanche deposit behind the natural lava-dam barrier of the waterfall (Reyes et al. 2021). A following change of the course of the River Coca further initiated regressive erosion upstream of the San Rafael waterfall (Ortiz et al. 2021; Reyes et al. 2021). Since then, ongoing mass movements along the River Coca put infrastructure, environment and indigenous communities at risk with cascading impacts considering the damage of national oil pipes located in the affected area. The oil infrastructure is further of high importance for the country's oil exportation and thereby the economy. Broken oil pipes affected the land of the Kichwa population, one of the 12 national tribes, shortly after the disappearance of the San Rafael waterfall (Bravo Díaz 2021). Since then, large vegetated areas are eroding. Furthermore, the erosion is approaching and threatening the Coca Codo Sinclair Dam, a hydroelectric power plant built in 2016 which has a capacity of 1500 MW (Terneus-Paez and Jiménez-Medoza 2019). The dam nowadays is supplying 25% of the national electricity demand (Agencia de Regulación y Control de Electricidad 2019). Current debates in Ecuador claimed that the construction of the hydroelectric plant is related to the collapse of the San Rafael waterfall and has influenced the regressive erosion process of the River Coca (Bernal 2017; Holtgrieve and Arias 2022). The damage caused by ongoing river erosion will make Ecuador face a drop in its national electricity supply.

Monitoring attempts are ongoing to protect the region and the renewable energy provision of the country. Therefore, landslide monitoring is crucial for fast disaster risk

management response in the region, especially in areas of multidimensional risk like the northeastern region of Ecuador. Understanding mass movements due to erosion in the region helps to develop an adequate risk assessment for landslide-prone areas such as the Andean region (Orejuela and Toulkeridis 2020). Landslides usually occur within a short period of time affecting the population and the environment in its direct proximity. Heavy rainfall periods and eventually flooding can further trigger landslides. Together with geologic structures and slope characteristics, they represent the main hazard components for landslide risk (Lee and Talib 2005; van Westen et al. 2003).

Remote sensing and Geographic Information Systems (GIS) play key roles for landslide risk monitoring. Geospatial analysis in a GIS allows the modeling of landslide susceptibility considering multiple causative factors. Assessment of landslide susceptibility can be conducted with Fuzzy Membership Function (Kirschbaum et al. 2016; Stanley and Kirschbaum 2017), Analytical Hierarchy Process (AHP) (Bahrami et al. 2021; Ghorbanzadeh et al. 2018) or Weighted Linear Combination (WLC) (Jabbar et al. 2019), or the mentioned in combination. Resulting maps help to identify areas exposed to landslides and provide insights with regard to the dynamics triggering an event. However, these models were rather developed for small-scale assessments and a lack of high-resolution data limit the potential for in detail landslide susceptibility assessment. Remote-sensing time-series analysis can further assist the monitoring of landslides and their impacts especially in regions with a high susceptibility to landslides. Here, remote but especially fast monitoring is crucial.

Mass movements are often related to heavy rainfall events. Dense cloud cover restricts the use of optical data such as Landsat 8 or Sentinel-2 imagery especially in tropical regions. Sentinel-1 Synthetic Aperture Radar (SAR) can overcome these challenges and is well suited for landslide detection (Kyriou and Nikolakopoulos 2018). The use of SAR data allows observations in areas with intense cloud coverage as occurring in the tropics. With regard to landslide monitoring, in particular, SAR data also provide the potential to derive additional information on surface roughness and structure compared to optical remote-sensing data. Sentinel-1 has already been used extensively for landslide (Raspini et al. 2018; Tzouvaras et al. 2020) and also for landslide risk (Olen and Bookhagen 2018) monitoring. With SAR data, changes in surface roughness and dielectric properties can be investigated using their backscatter information in the context of incoherent change detections. Furthermore, complex values can be considered to investigate phase shifts in the context of coherent change detections or interferometry (Jung and Yun 2020). However, monitoring of mass movements is challenging in tropical forest environments due to a rapid and dense vegetation growth which restricts

the use of interferometric approaches (Razak et al. 2013; Washaya et al. 2018). Attempts have been made monitoring landslides with bi-temporal change detection (BCD) methods especially using optical data and SAR (Huang et al. 2020; Mondini et al. 2021; Qin et al. 2018). Besides, to our current knowledge, cloud-based sequential change detection (SCD) for landslide monitoring using SAR has not been used and integrated for landslide monitoring and management. SCD can represent a very fast method to identify landslides in near-real time depending on the availability of images in the cloud-based environment. However, it is also key to validate resulting maps to identify adequate methods for individual study areas. Landslide risk monitoring and management could benefit from these techniques especially in remote areas such as the Amazon rainforest in Ecuador which are in addition difficult to access.

Models for landslide early warning aim to reduce landslide-induced damage and assist in closing the gap of local landslide research in Latin America and the Caribbean (Sepúlveda and Petley 2015). In line with the Sendai Framework for Disaster Risk Reduction (SFDRR) and to support priority 1 ‘understanding disaster risk’, this research study will conduct landslide detection in the study region and its potential for disaster risk management and analyze the development of the ongoing erosion between the San Rafael waterfall and the Coca Codo Sinclair Dam using (i) a BCD with a principal component analysis (PCA) in comparison to (ii) an SCD in a cloud-computing based environment to provide opportunities for near-real-time monitoring of landslide developments. Detected areas are (iii) validated with high-resolution imagery and support the identification of and adequate monitoring method and further help to identify potential trigger variables in the study area. Knowing the impact of certain trigger variables can be integrated in national risk assessment by underlining areas exposed to landslide hazard. While steep slopes in combination with heavy rainfall or high soil moisture in the sub-surface can trigger landslides in an area, the presence of vegetation cover could consolidate the land mass (Kalsnes and Capobianco 2022; Prancevic et al. 2020; Yuliza et al. 2016). Therefore, this study aims to collaborate with the national disaster risk management in close cooperation with local experts.

## 2 Study Area

The study area is located in the Northeast of Ecuador (Fig. 1). It is surrounded by the provinces of Napo and Sucumbios, in the Subandean zone of Ecuador. In the North is the protected Cayambe-Coca National Park. The River Coca crosses the area with an average discharge of 290 m<sup>3</sup>/s (Programa de las Naciones Unidas para el Medio Ambiente 2018). Elevation levels reach 500–3600 m a.s.l. The highest point is the peak

of the stratovolcano Reventador, which belongs to a complex of aligned volcanoes with Pan de Azúcar, Sumaco, and Conos de Puyo. The last eruption period started in 2002. Since then, the Reventador volcano remains active. The lavas that characterized the volcanic complex are andesitic and basaltic-andesitic. The cone of elongated shape reaches slopes up to 34°. In the last massive eruption (2002), the cone lost 110 m of its altitude. Since then, volcanic activity has contributed to an increase of its extension up to the current size. Volcanic rocks of the Misahualli Formation constitute the basement of the area. Lava flows, pyroclastic material flows, avalanche deposits, and lahars result from the eruptions of the Reventador Volcano. The upper layer over which the River Coca circulates is highly dynamic. Cycles of deposition and erosion currently form layers of materials with high heterogeneity and optimal conditions for water infiltration.

Humid montane forests cover the majority of the area. The precipitation increases toward the Amazon basin and ranges from 3000 to 6000 mm mean annual precipitation (MAP) with a gradient from East to West. The average temperature is 20 °C. The region is a megadiverse hotspot surrounded by a national park, Cayambe-Coca, and a worldwide recognized UNESCO biosphere reserve, Sumaco. Besides the economic importance of the study area for their natural resources, such as oil and energy, it has a valuable biological and cultural richness under the protection of the national law and international agreements.

## 3 Data and Methods

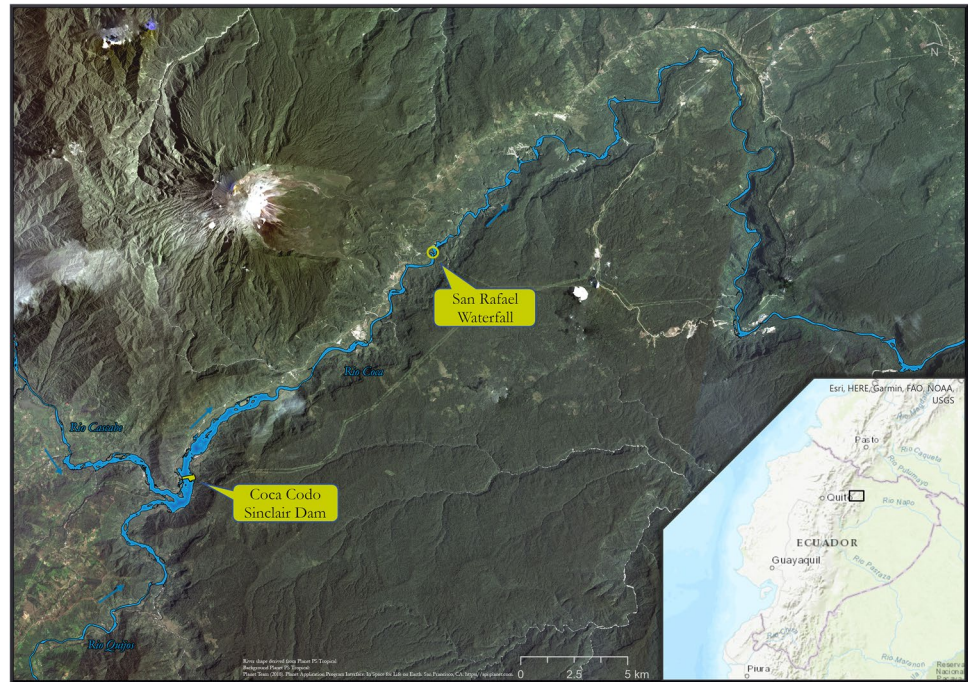
Landslide occurrence monitoring and assessments of the actual event were analyzed using Sentinel-1 SAR data and validation of detected changes assessed with high-resolution (HR) optical images between 2020-02-14 and 2020-03-2021. Based on the identified landslide detection approach, trigger variables were identified by the analysis of classified training samples into landslide and non-landslide samples.

### 3.1 Data

#### 3.1.1 Sentinel-1 SAR Data

Rainfall in the study area is high during the whole year, while additionally high cloud cover is present. SAR data, from an active remote sensor, allows monitoring during day and night and under all weather conditions. The detection of occurred landslides is based on Sentinel-1 Level-1 Ground Range Detected (GRD) images with Interferometric Wide Swath (IW) mode from 2020-02-14 to 2020-03-2021 with a temporal resolution of ~6 days and a spatial resolution of 20 m. This period was chosen based on the main landslide activities with regard to the regressive

**Fig. 1** Study area at the River Coca between the San Rafael Waterfall and the Coca Codo Sinclair Hydropower Dam. Background Image: Biannual PS Tropical Basemap from December 2019 to June 2020



erosion along the River Coca. Level-1 Ground Range Detected (GRD) products which are multi-looked and terrain corrected were preferred and the IW mode allows for dual polarization with a spatial resolution of 5 by 20 m. Single and Dual polarization modes were considered, i.e., co-polarization with VV, often used for soil moisture or flood monitoring (Martinis et al. 2018; Tsyganskaya et al. 2018) and cross-polarization with VH, which supports the monitoring of soil properties also in combination with VV (Canty et al. 2020; Periasamy 2018; Yang and Guo 2019).

### 3.2 3.1.2 High-Resolution Imagery

Results were validated in close exchange with local experts, comparisons with local assessment reports by CELEC SUR, as well as with high-resolution imagery. High-resolution reference data were generated from a PlanetScope image acquired on 2021–02–14, which represents the latest cloud free image at the time of the validation. Included is also the PS Tropical Normalized Analytic Biannual Archive basemap from June to November 2019 representing the reference image prior to the erosion. Data specifications are listed in Table 1.

#### 3.2.1 Landslide Hazard Assessment

For the identification of potential trigger variables, we integrated data on slope, land-cover density, sub-surface soil moisture and precipitation (Table 2). These variables are important to be included for further risk assessment and can guide national risk monitoring and management frameworks.

Data on slopes were based on the NASA Shuttle Radar Topography Mission (SRTM) (Farr et al. 2007) with 30 m spatial resolution. Data on the Enhanced Vegetation Index (EVI) were derived from MODIS with 250 m resolution and MAP was based on the Climate Hazards Group Infrared Precipitation with Station data (CHIRPS) (Funk et al. 2015). EVI data were preferred over the Normalized Difference Vegetation Index (NDVI) due to the monitoring over high biomass regions (Jiang et al. 2008). CHIRPS data are available on a daily basis with 4 km spatial resolution. With regard to in detailed assessment of precipitation records in the study area, a peak in rainfall amounts could be spotted toward the end of January 2020 when considering daily precipitation records. This heavy rainfall event could have been one of the causative factors for the erosion at the San Rafael waterfall. Nevertheless, monthly precipitation rates have large variations throughout the year and are common. Surface and sub-surface soil moisture information was derived from the NASA-USDA Enhanced SMAP Global Soil Moisture Data with a 3-day temporal and a 10 km spatial resolution (O'Neill et al. 2016).

## 3.3 Methods

### 3.3.1 Radar-Based Landslide Monitoring

Aiming at near real-time monitoring of landslides in densely vegetated areas leads to the identification of two approaches based on SAR imagery over the defined observation period: (i) BCD analysis based on PCA and (ii) SCD using a

**Table 1** Data specifications of landslide monitoring

Data	Time	Resolution	Source
Sentinel-1 GRD IW	14/02/20—16/03/21	20 m	Copernicus
PS Tropical Normalized Analytical Biannual Archive Basemap (Reference)	06/2019 – 11/2019	3 m	Planet
PlanetScope (Validation)	14/02/2021	3 m	Planet

**Table 2** Data for landslide hazard assessment

Data type	Dataset	Resolution	Source
Slope	NASA SRTM	30 m	Farr et al. (2007)
EVI	MODIS MOD13Q1	250 m	Didan (2015)
Precipitation	CHIRPS	4 km	Funk et al. (2015)
Soil moisture	NASA-USDA Enhanced SMAP Global Soil Moisture Data	10 km	Bolten et al. (2010); O'Neill et al. (2016); Sazib et al. (2018)

cloud-computing environment. The integration of Planet-lab imagery with 3 m resolution allowed validation of our results for both approaches. Figure 2 shows the workflow of the BCD and SCD approach.

#### *Bi-temporal Change Detection (BCD) with PCA*

Analysis of the first approach was performed with the Sentinel Application Platform (SNAP). All relevant data between the defined period in a 12-day interval were downloaded. After creation of a subset to minimize the data load to the study area, the orbit filter was applied in SNAP. The next two steps of pre-processing included the radiometric calibration and the speckle filtering. Radiometric calibration relates the pixel values to the radar backscatter of the selected scene. The calibration leads to a correction of radiometric disturbances and an atmospheric correction (Filippini 2019). Speckle filtering removes the speckled structures that usually appear in radar images. The origin of these structures is phase differences in the backscattered signal. Speckle filtering was used to remove image noise using a filter matrix (in this case a  $5 \times 5$  filter matrix) which overwrites the greyscale values. This helps to reduce the overestimation of the detected changes (Filippini 2019). The final pre-processing step was represented by geocoding using the Range-Doppler Terrain Correction in SNAP. This process provides a correction of distortions, for example, due to lateral shots from the satellite sensor. In addition, Range-Doppler Terrain Correction applies a digital elevation model (i.e., NASA SRTM with 90 m resolution) (Jarvis et al. 2008) and a coordinate system to correctly align the satellite image before the change detection (Filippini 2019).

After the pre-processing, respective data pairs can be passed on to the change detection assessment. In this case, both polarizations (VV + VH) were used and could be compared after completion (Asokan and Anitha 2019). For

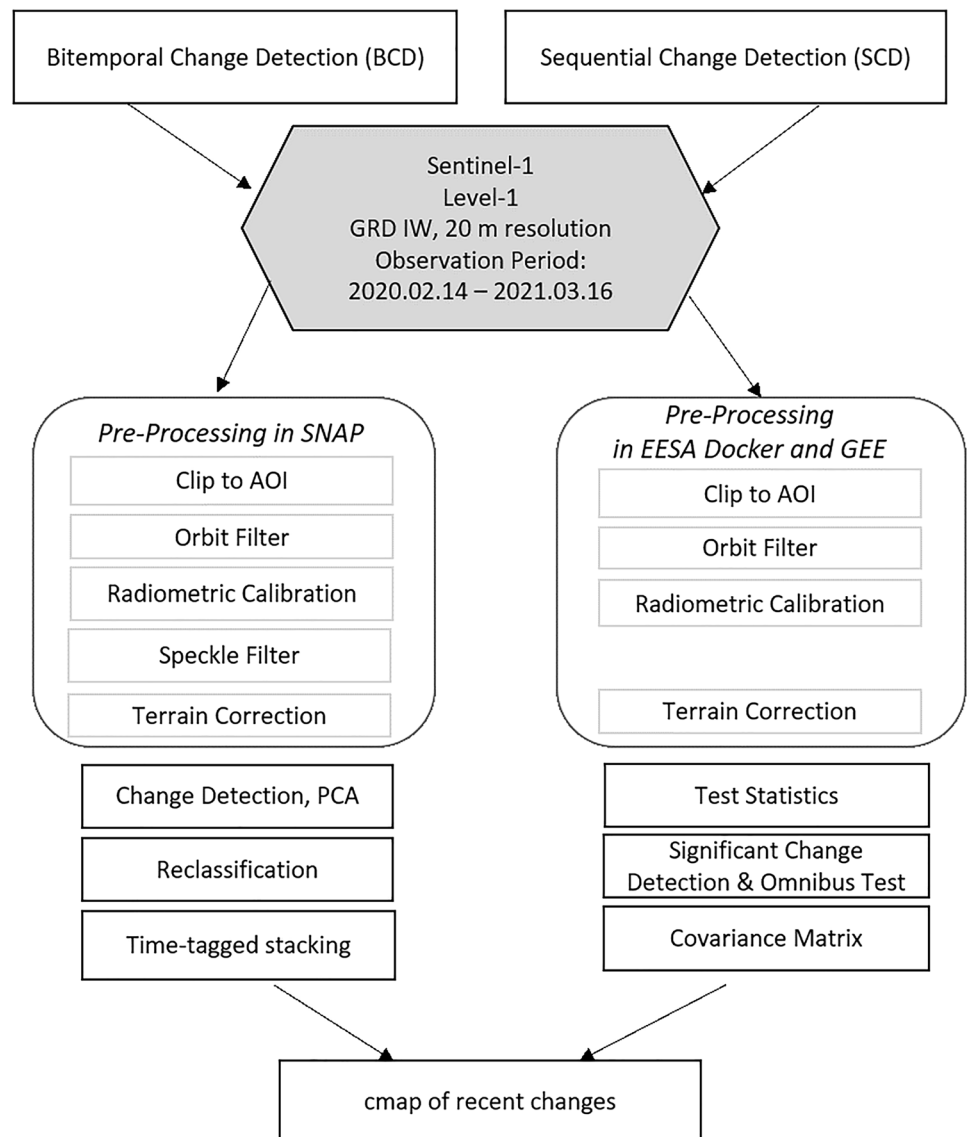
comparison of both results, a PCA is carried out. A PCA can be used for this purpose as it only allows the integration of those weighted values into the final product, which have the highest correlation and the highest significance to each other but also show the highest probability for visualization of the correct eroded areas. Furthermore, the PCA removes scatter and noise (Asokan and Anitha 2019). Moreover, the PCA results in new principal component images which allows datasets to be more simplified and illustrated by approximating a large number of statistical variables using a smaller number of linear combinations.

The spatio-temporal development of the detected changes was visualized considering the most recent changes in time (cmap). The single PCA images were turned into binary (change, no change) images using a threshold. With a combination of a Python script and QGIS, the binary images were turned into raster files with a single value (between 1 and 32), which is reliant on the image's position in time. During the stacking process of these 'time-tagged' single-value images, the highest pixel value of each position is considered, resulting in a single band 'cmap'. Finally, we masked out permanent water bodies using the JRC Global Surface Water data set (Pekel et al. 2016).

#### *Sequential Change Detection (SCD)*

An efficient approach to monitor regressive erosion using remote-sensing data at spatio-temporal scales is the Sequential Change Detection (SCD) as described by Conradsen et al. (2016) and Canty et al. (2020). We used the EESAR Docker Container provided by Canty (2021) and conducted the SCD using the Google Earth Engine (GEE) cloud-computing environment for the processing of 32 Sentinel-1 B GRD images in its 120<sup>th</sup> ascending orbit between the observation period. Analysis for dual polarization, VV and VH, was similar to the BCD approach. For the sequential SAR

**Fig. 2** Workflow of BCD and SCD approach with Sentinel-1 time-series data



change detection, especially multi-temporal polarimetric SAR data were considered. On a per-pixel basis, the technique identifies if a change occurred at a defined significance level between two SAR images taking into consideration the full time-series starting with the first image and ending with the most recent one (Canty et al. 2020). With a test statistic, p values are generated for each observation and a change map is then generated based on the testing of p values against the defined significant level (Canty et al. 2020). For this study, the analysis was carried out with a significance level of 0.01. By integrating the omnibus test (Nielsen et al. 2017), the identification of changes in a pixel can be conducted and updated. Besides the bands containing the changes between the intervals (bmap), the resulting raster dataset includes a band with the time of most recent changes (cmap), the time of first change (smap) and another band with the total number of registered changes (fmap). For

analysis, the cmap was chosen, and to remove water level-related changes, we also masked out permanent waterbodies using the JRC Global Surface Water data set.

#### Validation

Based on the HR imagery included for validation (see Sect. 3.1.2), the bands with the changes between the observation period were extracted and vectorized for validation. For the purpose of a first validation with additional data based on expert information, we reduced the validation area to a river section of approximately 7.8 km close to where the San Rafael waterfall was located. We then combined the results of the BCD and the SCD with the digitized eroded areas derived from the HR imagery and computed a confusion matrix based on the true-positive, true-negative, false-positive and false-negative areas.

### Landslide Hazard Detection

Based on the landslide detection with Sentinel-1 potential variables for hazard were monitored over the considered time period with time-series analysis in GEE and R. Sample areas of non-landslide detected areas were further included to detect differences in the variable behavior compared to those where landslides could be detected and validated. Daily data on precipitation were averaged over 3 days for a timely overlap with the 3-day average soil moisture information.

## 4 Results

### 4.1 Comparison of the BCD and SCD Approach

Figure 3 shows the occurrence of changes with both approaches by visualizing the cmap results referring to changes over the observed time period 2020-02-14 to 2021-03-16 focusing on the most recent changes in the study area. While the BCD detected an area of 355.9 km<sup>2</sup> being affected by changes that could refer to landslides, the SCD identified 420.9 km<sup>2</sup> within the whole study area. Around 66.51% of all pixels identified in the SCD overlapped with those detected in the BCD, while the BCD showed only an overlap of 42.76% with the SCD approach. In addition, we could also detect multiple pixels off the main regressive erosion area at the River Coca being located close to Volcano Reventador with the BCD approach.

Validation with HR data was conducted for a smaller area along the lower part of River Coca (see also Fig. 3). Insights in the visual comparison are given as an example in Fig. 4 where PlanetScope Basemaps before and after the erosion are compared with resulting maps out of the SCD approach.

*Validation* As we focus on regressive river erosion along the River Coca, the validation area was digitized with a 650 m buffer along the river to identify false and true positives as well as false and true negatives in both landslide detection approaches. Figure 5 shows the spatial validation of both approaches and highlights a 67.19% larger area of true positives for the SCD approach. About 75.31% of detected changes detected by the SCD were further identified as true positive, while only 58.54% of the BCD were identified as true positive.

According to the confusion matrix, the BCD got an overall accuracy of 0.89, a sensitivity of only 0.44, and a specificity of 0.97, while the SCD has a sensitivity of 0.75, a specificity of 0.94, and an overall accuracy of 0.91 (Table 3).

*Potential Variables for Landslide Risk Monitoring* Results of the BCD and the validation map were used as input data for the landslide detection areas to be compared with potential trigger variables. The identification of trigger variables

helps to build a comprehensive risk assessment with regard to landslide monitoring and management in the region considering the given preconditions. Besides the EVI, precipitation rates and soil moisture data, only the integration of slope information was not included in a dynamic manner.

*Slope* We could observe an overlap of higher slopes with landslides especially in the early stages of the regressive erosion. Toward the starting of the regressive erosion from 2020-02-14 to 2020-03-21, we can detect rather lower slope values similar to those values in the non-landslide detected areas.

*Precipitation and Soil Moisture* Precipitation rates were observed over the whole time period based on CHIRPS data. A peak can be measured by begin of February which overlaps with the start of the regressive erosion on 2 February and the disappearance of the San Rafael waterfall. Figure 7 shows precipitation and sub-surface soil moisture plots with a trend for the observation period in the study area for landslide detected areas (Fig. 7a) as well as non-landslide detected areas (Fig. 7b).

While the variability of precipitation is similar in both areas, precipitation rates and the trend of precipitation in the observation period are slightly higher in the landslide detected areas.

Sub-surface soil moisture according to the considered data is higher in the non-landslide detected areas. Even by considering a coarse resolution of 10 km, higher soil moisture levels could lead to an increase of landslide hazard in the region.

Based on high precipitation rates during the start of the regressive erosion, further all pixels of the SCD were plotted with maximum precipitation rates over the whole time period and could indicate a relationship between the occurrence of rainfall with maximum precipitation rates (Fig. 8).

*Vegetation* As a dense vegetation cover might stabilize the soil and could thereby reduce the risk for landslides, we expected a relationship between vegetation productivity (represented by EVI) and landslide, respectively, non-landslide areas. EVI profiles of landslide and non-landslide detection areas did not indicate a dense relationship with landslides as only small differences could be identified (Fig. 9). In the beginning of the erosion, EVI profiles show higher values in the non-landslide areas, but with regard to the full observation period, a clear relationship cannot be identified.

## 5 Discussion

Landslide monitoring in the study area is crucial to support national risk management. As landslides represent a fast hazard, near real-time monitoring techniques are

## Regressive Erosion at the Coca River, Ecuador

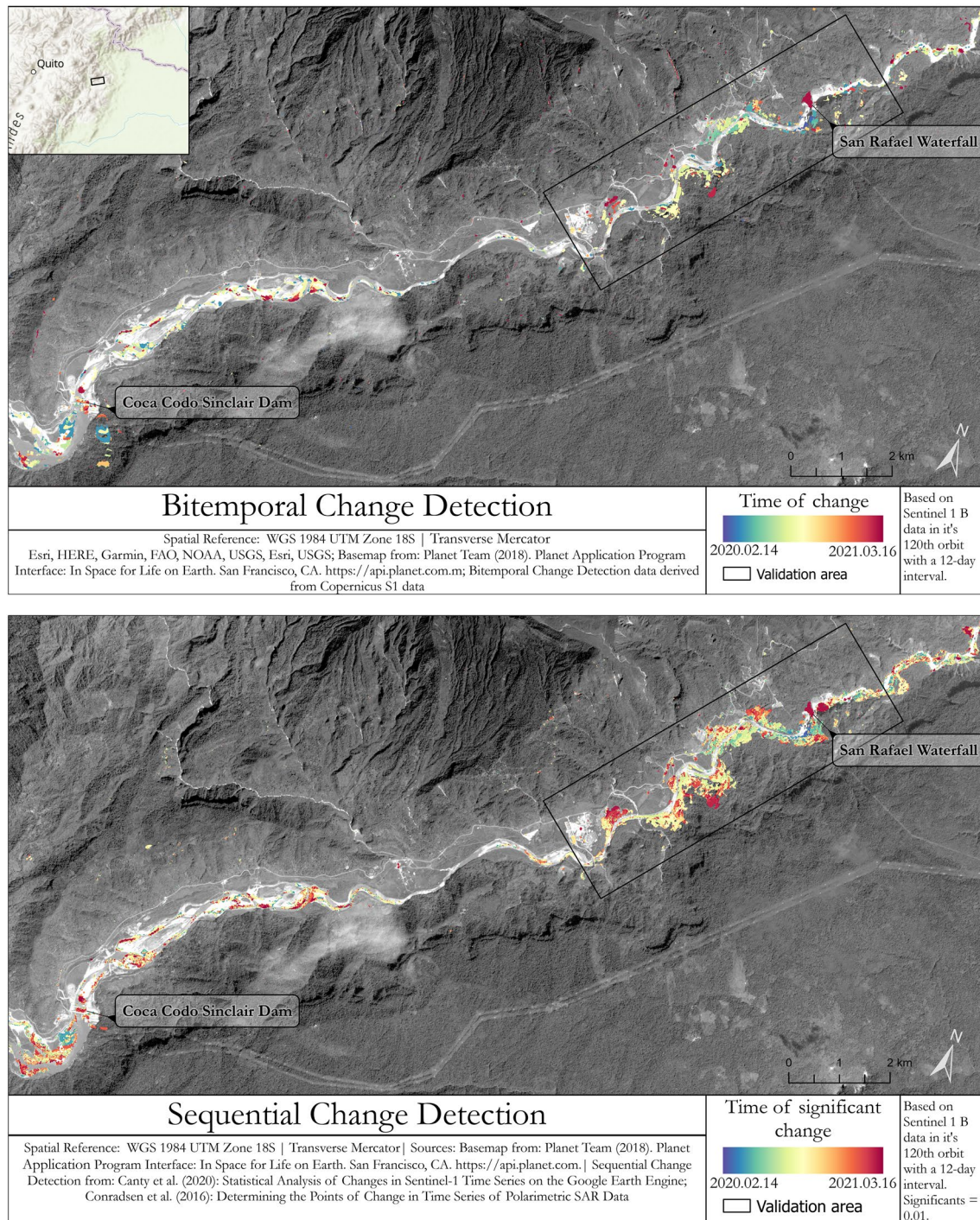


**Fig. 3** Landslide detection with the **a** bi-temporal change detection approach (BCD) and the **b** sequential change detection approach SCD based on Sentinel-1 time-series data between 2020-02-14 and 2021-03-16. The black box shows the area used for validation

needed. However, also pro-active action is required which demands a comprehensive understanding of landslide risk and dynamics of causative factors. Understanding landslide

movements and their development helps to train models for early warning mechanisms.

The use of Sentinel-1 and thereby SAR data is necessary due to high cloud coverage and detection of surface

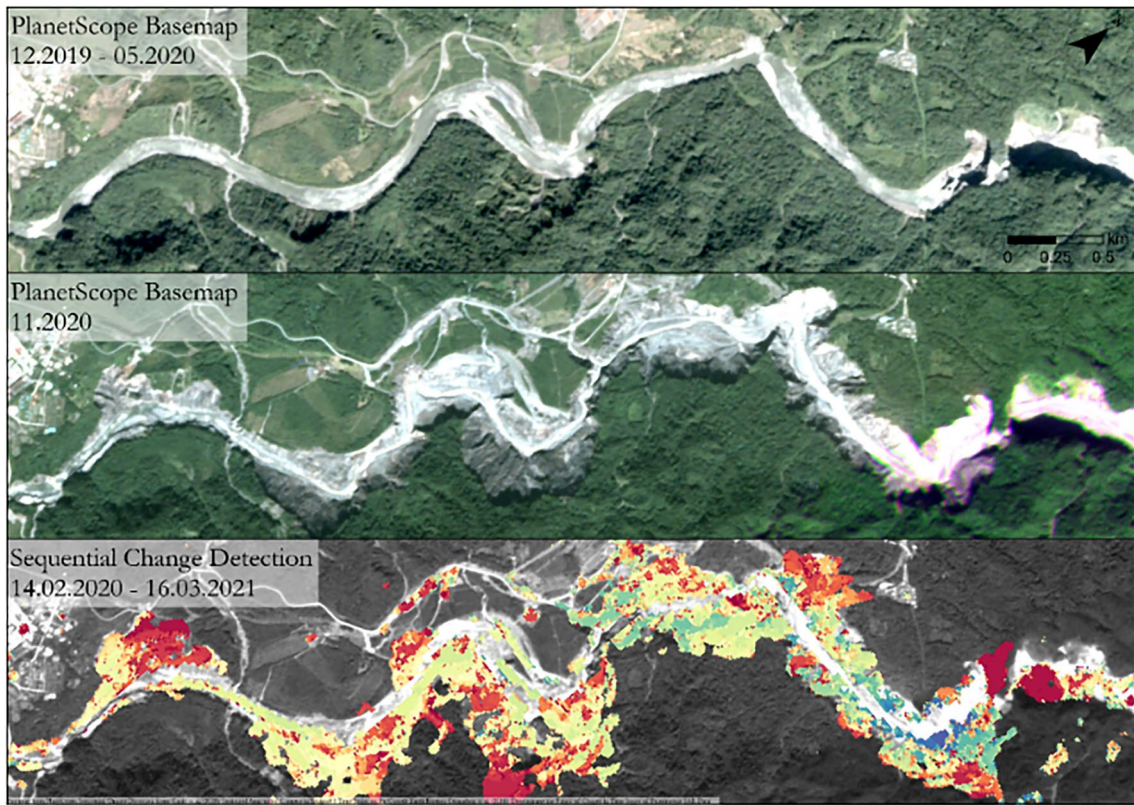


Fig. 4 Validation of the northwestern segment of the beginning regressive erosion for visual comparison

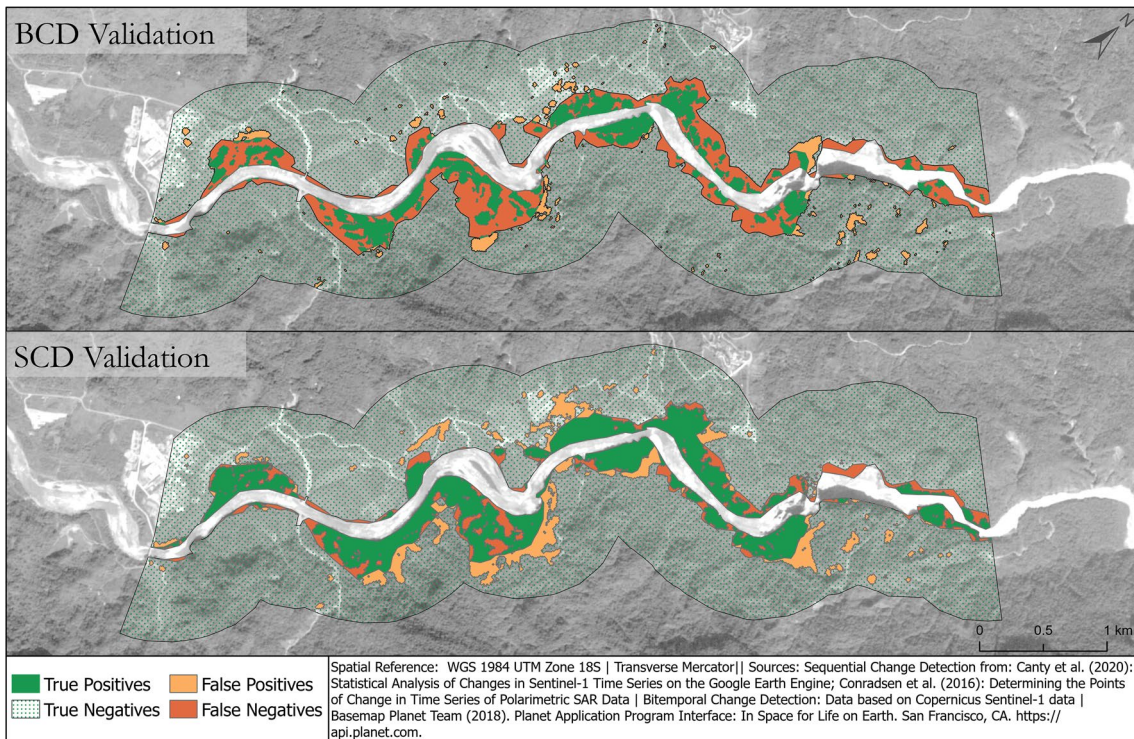
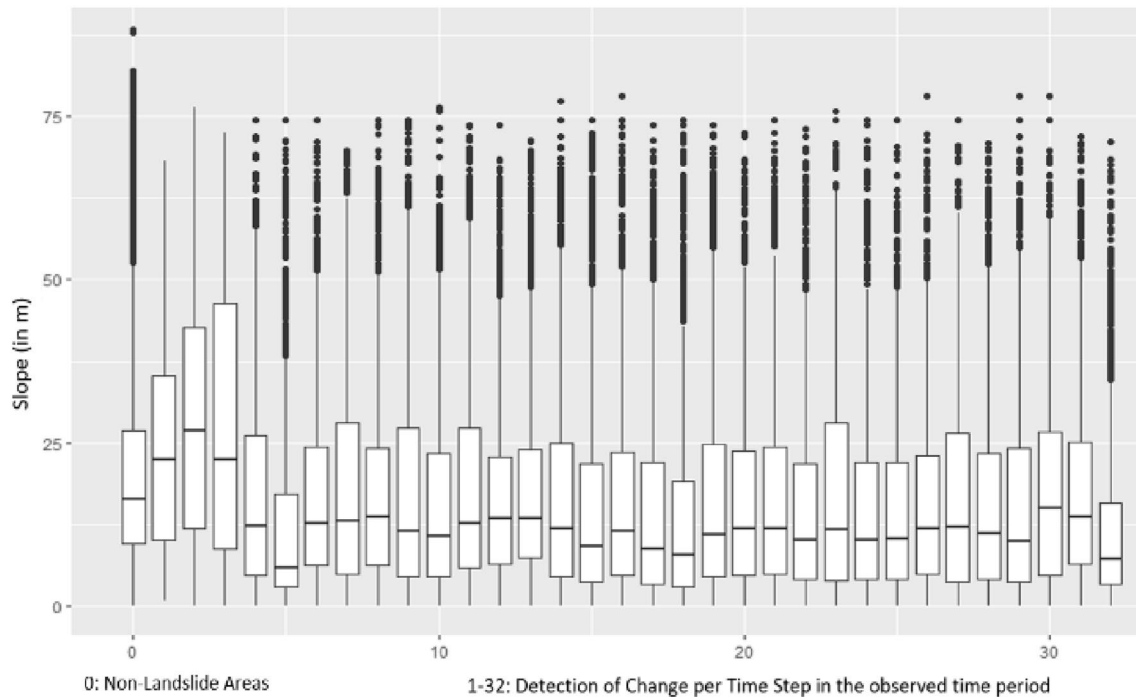


Fig. 5 Validation area (as shown in Fig. 6) for both the BCD and the SCD approach with regard to the digitized reference data using HR imagery by PlanetScope



**Fig. 6** Boxplot showing the single landslide detection time steps compared to slope values in the study region

parameters. Nevertheless, monitoring of landslides with SAR data is still challenging in tropical regions. An Interferometric Coherence Difference (ICD) technique was used in the presented study which focused on the backscattering signal caused by rough surfaces such as bare soil and steep slopes. Coherent Change Detection (CCD) techniques were tested by including interferometric information, but results were misleading due to a highly dense vegetation cover in the tropical Andean region of the River Coca.

The presented results allow for near real-time monitoring with Sentinel-1 time-series with a spatial resolution of 20 m and a 6-day temporal resolution. BCD helped to identify specific movements during fixed time intervals with an overall accuracy of 0.88, while the SCD approach, run in a cloud-based environment, represents a more time-efficient analysis of landslide detection and allows for a higher accuracy of 0.91 compared to the BCD. Validation areas have been included but could be expanded for further analysis.

**Table 3** Accuracy assessment based on HR imagery

	Bi-temporal CD	Sequential CD
Sensitivity	0.370	0.752
Specificity	0.974	0.942
Accuracy	0.879	0.912

CD change detection

Nevertheless, optical reference data cannot replace field validation data and might contribute to error propagation in the validation processes, especially as the acquisition times of PlanetScope do not match accurately with the revisit time of Sentinel 1B. Thus, the SCD's tendency to over-prediction could be the result of uneven recording dates (reference data from 2021-02-14 and SCD data from 2021-02-20). Moreover, the manually digitized eroded areas in the reference images might have been inaccurate in some parts and do not depict the reality on the ground.

With regard to the validation area where we integrated HR imagery and digitized patterns of erosion to identify the pixels that were classified correctly, we could identify the SCD as the better approach due to a 67.19% bigger area classified as 'true positive' compared to the BCD approach.

Potential trigger variables could be identified such as steeper slopes in the areas where the regressive erosion started as well as increasing precipitation and sub-surface soil moisture rates in the landslide detected regions. Profiles of EVI in the areas were not showing a significant relationship to landslides. Here, analysis per time step could be relevant as spatial and temporal autocorrelation has to be considered. While landslides seem to be triggered by topographic preconditions and kept ongoing due to biophysical dynamic variables, nevertheless, additional factors, such as mining activities, whether legal or illegal, at the origin of the erosion should be considered as well and integrated

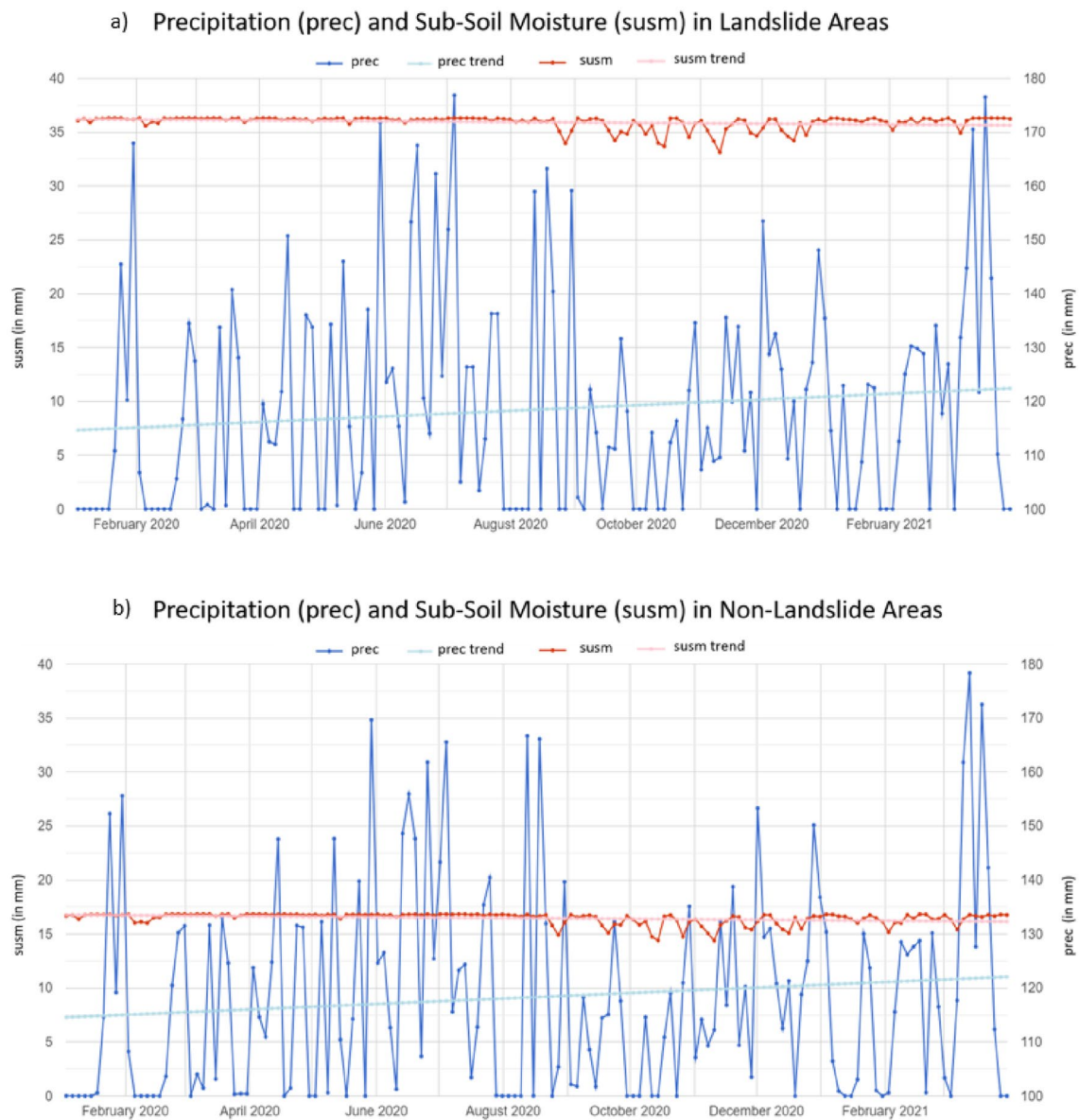


**Fig. 7** Time Series analysis over **a** landslide and **b** non-landslide detection areas for precipitation and sub-surface soil moisture

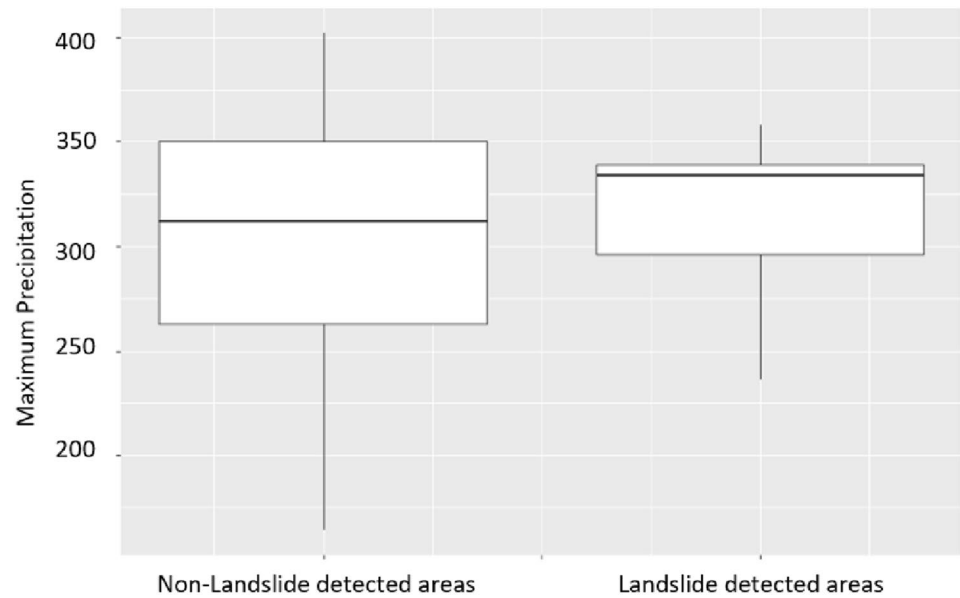
in hazard and risk mapping approaches. To improve the assessment of landslide variables, higher resolution data on precipitation but also soil moisture would be important to integrate.

The here presented approach shows how landslide risk could be assessed in near-real time considering a sequential time-series analysis in a cloud-based environment. Furthermore, information on explanatory variables in a timely manner to allow for dynamic variations should be considered. Similar to drought events where the standardized

precipitation index (SPI) which is often used as an indicator of drought hazard when values are below 0, an increase in precipitation over a short time could be embedded in a dynamic modeling of landslide hazard.

Fast toward near real-time monitoring using SAR data helps to support early warning mechanisms. In close exchange with local and regional experts, the monitoring of landslide risk can be guided toward pro-active action, including suitability assessments for future infrastructure construction and stability measures.

**Fig. 8** Maximum precipitation rates in non-landslide and landslide detected areas



**MODIS EVI Profile over Landslide and non-Landslide Areas**



**Fig. 9** EVI profiles in landslide and non-landslide detection areas

## 6 Conclusions

The risk of landslides leading to environmental and socio-economic damage is high in the presented study area. Infrastructural damage with regard to roads but especially key infrastructure for Ecuador's economy and energy such as oil pipes and the Coca Codo Sinclair Dam are of high national interest. Landslides along the River Coca in direct proximity to the dam but especially with already destroyed main oil pipes lead to cascading effects of an already ongoing

disaster. Oil spills occurred in the study region in April 2020 and January 2022 due to broken oil pipes originated from mudslides, affect indigenous people and their lands, and have various impacts on the social, economic and environmental dimension threatening sustainable development in many facets. Protection of indigenous knowledge and indigenous communities in affected areas should, therefore, be part of the national strategy for pro-active risk management across scale. Latin American countries, such as Ecuador, have a high dependence on hydropower generation, a clean source of energy, which is in line with the Agenda 2030

and SDG 7 but which makes the country's electricity supply highly vulnerable to natural hazards. These hazards, landslides being among them, are also expected to be worsened by climate change. In the here presented study, a method for fast landslide monitoring using an SCD analysis could be identified. By comparing results from the BCD and the SCD validated with high-resolution imagery, higher accuracies of the SCD with 0.91 compared to 0.88 of the BCD were identified. In addition, a much faster processing due to the application in a cloud-base environment represents a high potential for landslide risk monitoring and management in the region. The SCD promotes a continuous analysis over the time-series, and does not compare binary images only, but considers the trend over all images from the time-series. The analysis of trigger variables showed partly some expected results such as the close relationship between slope or soil moisture and landslides, but could not identify a close relationship, e.g., between vegetation cover and landslides. The selected method could become an important asset for the operation of power plants, guarantees security of energy supply, and strengthens the improvement of protection mechanisms of the society, the economy and the environment. Further research embeds the here presented methods to identify landslide hazard, vulnerability and exposure variables to create risk profiles for the region.

**Acknowledgements** We highly acknowledge the support by our Ecuadorian colleagues and experts who guided the selection of variables and provided in detail explanations for the ongoing dynamics in the study region. Also, we acknowledge support by the DFG Open Access Publication Funds of the Ruhr-Universität Bochum.

**Author contributions** Conceptualization, susceptibility analysis, methodology, writing, investigation and coordination of contributions were conducted by VG, Analysis of the sequential change detection and description was done by TD, Analysis of the bi-temporal change detection and description was conducted by RH. Data provision and support, local knowledge exchange and editing according to local validation and expert assessment were done by PG and JJ, Supervision editing and writing was conducted by CJ. All authors reviewed and edited the manuscript, and all authors have read and agreed to the published version of the manuscript.

**Funding** Open Access funding enabled and organized by Projekt DEAL.

**Open Access** This article is licensed under a Creative Commons Attribution 4.0 International License, which permits use, sharing, adaptation, distribution and reproduction in any medium or format, as long as you give appropriate credit to the original author(s) and the source, provide a link to the Creative Commons licence, and indicate if changes were made. The images or other third party material in this article are included in the article's Creative Commons licence, unless indicated otherwise in a credit line to the material. If material is not included in the article's Creative Commons licence and your intended use is not permitted by statutory regulation or exceeds the permitted use, you will need to obtain permission directly from the copyright holder. To view a copy of this licence, visit <http://creativecommons.org/licenses/by/4.0/>.

## References

- Agencia de Regulación y Control de Electricidad (2019) Estadística Anual y Multianual del Sector Eléctrico Ecuatoriano
- Asokan A, Anitha J (2019) Change detection techniques for remote sensing applications: a survey. *Earth Sci Inform* 12(2):143–160. <https://doi.org/10.1007/s12145-019-00380-5>
- Bahrami Y, Hassani H, Maghsoudi A (2021) Landslide susceptibility mapping using AHP and fuzzy methods in the Gilan province, Iran. *GeoJournal* 86(4):1797–1816. <https://doi.org/10.1007/s10708-020-10162-y>
- Bernal IC (2017) Informe Final Proyecto PIMI14–09. Quito-Ecuador: Escuela Politécnica Nacional
- Bolten J, Crow W, Zhan X, Jackson T, Reynolds C (2010) Evaluating the utility of remotely sensed soil moisture retrievals for operational agricultural drought monitoring. *IEEE J Sel Top Appl Earth Obs Remote Sens* 3(1):57–66. <https://doi.org/10.1109/JSTARS.2009.2037163>
- Bravo Díaz A (2021) “Sumak Kawsay Is Harmful for All of Us”: oil roads and well-being among the Waorani in Ecuadorian Amazonia. *Latin Am Perspect* 48(3):51–68. <https://doi.org/10.1177/0094582X211004909>
- Canty M (2021) EESAR Docker container. <https://github.com/mortcanty/EESARDocker>
- Canty M, Nielsen A, Conradsen K, Skriver H (2020) Statistical analysis of changes in Sentinel-1 time series on the Google earth engine. *Remote Sens* 12(1):46. <https://doi.org/10.3390/rs12010046>
- Carvajal P, Anandarajah G, Mulugetta Y, Dessens O (2017) Assessing uncertainty of climate change impacts on long-term hydropower generation using the CMIP5 ensemble—the case of Ecuador. *Clim Change* 144(4):611–624. <https://doi.org/10.1007/s10584-017-2055-4>
- Conradsen K, Nielsen A, Skriver H (2016) Determining the points of change in time series of polarimetric SAR data. *IEEE Trans Geosci Remote Sens* 54(5):3007–3024. <https://doi.org/10.1109/TGRS.2015.2510160>
- Didan K (2015) MOD13Q1 MODIS/Terra vegetation indices 16-day L3 global 250m SIN Grid V006
- Dille M, Chen R, Deichmann U, Lerner-Lam A, Arnold M (2012) Natural disaster hotspots: a global risk analysis. Washington, DC, World Bank. <https://www.openknowledge.worldbank.org/handle/10986/7376License:CCBY3.OIGO>
- EM-DAT (2022) The emergency events database
- Farr T, Rosen P, Caro E, Crippen R, Duren R, Hensley S, Kobrick M, Paller M, Rodriguez E, Roth L, Seal D, Shaffer S, Shimada J, Umland J, Werner M, Oskin M, Burbank D, Alsdorf D (2007) The shuttle radar topography mission. *Rev Geophys*. <https://doi.org/10.1029/2005RG000183>
- Filippini F (2019) Sentinel-1 GRD preprocessing workflow. *Proceedings* 18(1):11. <https://doi.org/10.3390/ECRS-3-06201>
- Funk C, Peterson P, Landsfeld M, Pedreros D, Verdin J, Shukla S, Husak G, Rowland J, Harrison L, Hoell A, Michaelsen J (2015) The climate hazards infrared precipitation with stations—a new environmental record for monitoring extremes. *Sci Data* 2:150066. <https://doi.org/10.1038/sdata.2015.66>
- Ghorbanzadeh O, Feizizadeh B, Blaschke T (2018) An interval matrix method used to optimize the decision matrix in AHP technique for land subsidence susceptibility mapping. *Environ Earth Sci*. <https://doi.org/10.1007/s12665-018-7758-y>
- Greiving S, Schödl L, Gaudry K-H, Quintana Miralles I, Prado Larraín B, Fleischhauer M, Jácome Guerra M, Tobar J (2021) Multi-risk assessment and management—a comparative study of the current state of affairs in Chile and Ecuador. *Sustainability* 13(3):1366. <https://doi.org/10.3390/su13031366>

- Guns M, Vanacker V (2013) Forest cover change trajectories and their impact on landslide occurrence in the tropical Andes. *Environ Earth Sci* 70(7):2941–2952. <https://doi.org/10.1007/s12665-013-2352-9>
- Holtgrieve GW, Arias ME (2022) Optimizing Amazonian dams for nature. *Science* 375(6582):714–715
- Huang Q, Wang C, Meng Y, Chen J, Yue A (2020) Landslide monitoring using change detection in multitemporal optical imagery. *IEEE Geosci Remote Sens Lett* 17:312–316. <https://doi.org/10.1109/LGRS.2019.291825>
- Jabbar F, Grote K, Tucker R (2019) A novel approach for assessing watershed susceptibility using weighted overlay and analytical hierarchy process (AHP) methodology: a case study in Eagle Creek Watershed, USA. *Environ Sci Pollut Res Int* 26(31):31981–31997. <https://doi.org/10.1007/s11356-019-06355-9>
- Jarvis A, Guevara E, Reuter H, Nelson A (2008) Hole-filled SRTM for the globe version 4 data grid
- Jiang Z, Huete A, Didan K, Miura T (2008) Development of a two-band enhanced vegetation index without a blue band. *Remote Sens Environ* 112(10):3833–3845. <https://doi.org/10.1016/j.rse.2008.06.006>
- Jung J, Yun S-H (2020) Evaluation of coherent and incoherent landslide detection methods based on synthetic aperture radar for rapid response: a case study for the 2018 Hokkaido landslides. *Remote Sens* 12(2):265. <https://doi.org/10.3390/rs12020265>
- Kalsnes B, Capobianco V (2022) Use of vegetation for landslide risk mitigation. [https://doi.org/10.1007/978-3-030-86211-4\\_10](https://doi.org/10.1007/978-3-030-86211-4_10)
- Kirschbaum D, Stanley T, Yatheendradas S (2016) Modeling landslide susceptibility over large regions with fuzzy overlay. *Landslides* 13(3):485–496. <https://doi.org/10.1007/s10346-015-0577-2>
- Kyriou A, Nikolakopoulos K (2018) Assessing the suitability of Sentinel-1 data for landslide mapping. *Eur J Remote Sens* 51(1):402–411. <https://doi.org/10.1080/22797254.2018.1444944>
- Lee S, Talib J (2005) Probabilistic landslide susceptibility and factor effect analysis. *Environ Geol* 47(7):982–990. <https://doi.org/10.1007/s00254-005-1228-z>
- Martinis S, Plank S, Ćwik K (2018) The use of Sentinel-1 time-series data to improve flood monitoring in arid areas. *Remote Sens* 10(4):583. <https://doi.org/10.3390/rs10040583>
- Mondini A, Guzzetti F, Chan K-T, Monserrat O, Martha T, Manconi A (2021) Landslide failures detection and mapping using synthetic aperture radar: past, present and future. *Earth Sci Rev*. <https://doi.org/10.1016/j.earscirev.2021.103574>
- Nielsen A, Conradsen K, Skriver H, Canty M (2017) Change detection in a series of Sentinel-1 SAR data. In: 2017 9th International workshop on the analysis of multitemporal remote sensing images (MultiTemp), p 1–3
- Olen S, Bookhagen B (2018) Mapping damage-affected areas after natural hazard events using Sentinel-1 coherence time series. *Remote Sens* 10(8):1272. <https://doi.org/10.3390/rs10081272>
- O'Neill P, Chan S, Njoku EG, Jackson T, Bindlish R (2016) SMAP L3 radiometer global daily 36 km EASE-grid soil moisture, version 4
- Orejuela I, Toulkeridis T (2020) Evaluation of the susceptibility to landslides through diffuse logic and analytical hierarchy process (AHP) between Macas and Riobamba in Central Ecuador. In: 2020 Seventh international conference on eDemocracy & eGovernment (ICEDEG), p 201–207
- Ortiz H, Matoza R, Johnson J, Hernandez S, Anzieta J, Ruiz M (2021) Autocorrelation infrasound interferometry. *J Geophys Res Solid Earth*. <https://doi.org/10.1029/2020JB020513>
- Pekel J-F, Cottam A, Gorelick N, Belward A (2016) High-resolution mapping of global surface water and its long-term changes. *Nature* 540(7633):418–422. <https://doi.org/10.1038/nature20584>
- Periasamy S (2018) Significance of dual polarimetric synthetic aperture radar in biomass retrieval: an attempt on Sentinel-1. *Remote Sens Environ* 217:537–549. <https://doi.org/10.1016/j.rse.2018.09.003>
- Prancevic J, Lamb M, McArdell B, Rickli C, Kirchner J (2020) Decreasing landslide erosion on steeper slopes in soil-mantled landscapes. *Geophys Res Lett*. <https://doi.org/10.1029/2020GL087505>
- Programa de las Naciones Unidas para el Medio Ambiente (2018) La economía de los ecosistemas y la biodiversidad-cuenca del Río Coca (Amazonía Ecuatoriana)
- Qin Y, Lu P, Li Z (2018) Landslide inventory mapping from bitemporal 10 m Sentinel-2 images using change detection based Markov random field. *ISPRS Int Arch Photogramm Remote Sens Spat Inf Sci XLII-3*:1447–1452. <https://doi.org/10.5194/isprs-archives-XLII-3-1447-2018>
- Raspini F, Bianchini S, Ciampalini A, Del Soldato M, Solari L, Novali F, Del Conte S, Rucci A, Ferretti A, Casagli N (2018) Continuous, semi-automatic monitoring of ground deformation using Sentinel-1 satellites. *Sci Rep* 8(1):7253. <https://doi.org/10.1038/s41598-018-25369-w>
- Razak K, Santangelo M, van Westen C, Straatsma M, de Jong S (2013) Generating an optimal DTM from airborne laser scanning data for landslide mapping in a tropical forest environment. *Geomorphology* 190:112–125. <https://doi.org/10.1016/j.geomorph.2013.02.021>
- Reyes P, Procel S, Sevilla J, Cabero A, Orozco A, Córdova J, Lima F, Vasconez F (2021) Exceptionally uncommon overburden collapse behind a natural lava dam: Abandonment of the San-Rafael Waterfall in northeastern Ecuador. *J South Am Earth Sci* 110:103353. <https://doi.org/10.1016/j.jsames.2021.103353>
- Sazib N, Mladenova I, Bolten J (2018) Leveraging Google earth engine for drought assessment using global soil moisture data. *Remote Sens* 10(8):1265. <https://doi.org/10.3390/rs10081265>
- Sepúlveda S, Petley D (2015) Regional trends and controlling factors of fatal landslides in Latin America and the Caribbean. *Nat. Hazards Earth Syst Sci* 15:1821–1833. <https://doi.org/10.5194/nhess-15-1821-2015>
- Stanley T, Kirschbaum D (2017) A heuristic approach to global landslide susceptibility mapping. *Nat Hazard* 87(1):145–164. <https://doi.org/10.1007/s11069-017-2757-y>
- Terneus-Paez F, Jiménez-Medoza S (2019) Nexa agua - energía: Análisis del flujo hídrico del Proyecto Hidroeléctrico Coca Codo Sinclair. *Ingenius* 21:53–62. <https://doi.org/10.17163/ings.n21.2019.05>
- Tibaldi A, Ferrari L, Pasquarè G (1995) Landslides triggered by earthquakes and their relations with faults and mountain slope geometry: an example from Ecuador. *Geomorphology* 11(3):215–226. [https://doi.org/10.1016/0169-555X\(94\)00060-5](https://doi.org/10.1016/0169-555X(94)00060-5)
- Tsuneki H, Guerrero R, Maricarmen E, Hiramatsu A, Deopersad C, Ishiwatari M, Minamitani T (2017) Lessons learnt from Japan and Latin America and Caribbean countries in management of hazard resilient infrastructure. A JICA-IDB Joint Research Environment. Rural Development and Disaster Risk Management Division
- Tsyganskaya V, Martinis S, Marzahn P, Ludwig R (2018) Detection of temporary flooded vegetation using Sentinel-1 time series data. *Remote Sens* 10(8):1286. <https://doi.org/10.3390/rs10081286>
- Tzouvaras M, Danezis C, Hadjimitsis D (2020) Small scale landslide detection using Sentinel-1 interferometric SAR coherence. *Remote Sens* 12(10):1560. <https://doi.org/10.3390/rs12101560>
- van Westen C, Rengers N, Soeters R (2003) Use of geomorphological information in indirect landslide susceptibility assessment.

- Nat Hazard 30(3):399–419. <https://doi.org/10.1023/B:NHAZ.0000007097.42735.9e>
- Washaya P, Balz T, Mohamadi B (2018) Coherence change-detection with Sentinel-1 for natural and anthropogenic disaster monitoring in urban areas. *Remote Sens* 10(7):1026. <https://doi.org/10.3390/rs10071026>
- Yang R-M, Guo W-W (2019) Using time-series Sentinel-1 data for soil prediction on invaded coastal wetlands. *Environ Monit Assess* 191(7):462. <https://doi.org/10.1007/s10661-019-7580-3>
- Yuliza E, Habil H, Munir MM, Irsyam M, Abdullah M, Khairurrijal K (2016) Study of soil moisture sensor for landslide early warning system: experiment in laboratory scale. *J Phys Conf Ser* 739:012034. <https://doi.org/10.1088/1742-6596/739/1/012034>